Jour. of Radiosurgery and SBRT, Vol. 4, pp. 191-201
Reprints available directly from the publisher
Photocopying permitted by license only

Clinical Investigation

Prospective evaluation of target and spinal cord motion and dosimetric changes with respiration in spinal stereotactic body radiation therapy utilizing 4-D CT

Xin Wang, PhD[1], Amol J. Ghia, MD[2], Zhongxiang Zhao, PhD[1], Jinzhong Yang, PhD[1], Dershan Luo, PhD[1], Tina M. Briere, PhD[1] , Ramiro Pino, PhD[3], Jing Li, MD, PhD[2], Mary F. McAleer, MD, PhD[2], David C. Weksberg, MD, PhD[4], Eric L. Chang, MD[5], Paul D. Brown, MD[2] and James N. Yang, PhD[1]

[1]Department of Radiation Physics, The University of Texas MD Anderson Cancer Center, Houston, TX, USA
[2]Department of Radiation Oncology, The University of Texas MD Anderson Cancer Center, Houston, TX, USA
[3]Department of Radiation Oncology, Houston Methodist Hospital, Houston, TX, USA
[4]Department of Radiation Oncology, PinnacleHealth Cancer Institute, Harrisburg, PA, USA
[5]Department of Radiation Oncology, University of Southern California Keck School of Medicine, Norris Cancer Hospital, Los Angeles, CA, USA

Correspondence to: James N. Yang, PhD, Department of Radiation Physics, Unit 1420, The University of Texas MD Anderson Cancer Center, 1400 Pressler St., Houston, TX 77030, USA; E-mail: jamesyang@mdanderson.org; Phone: +1 (713) 563-0164; Fax: +1 (713) 563-2545

(Received: May 26, 2016; Accepted: August 9, 2016)

Purpose: To assess the dosimetric effects of respiratory motion on the target and spinal cord in spinal stereotactic body radiation therapy (SBRT).

Methods and materials: Thirty patients with 33 lesions were enrolled on a prospective clinical protocol and simulated with both free-breathing and four-dimensional (4-D) computed tomography (CT). We studied the target motion using 4-D data (10 phases) by registering a secondary image dataset (phase 1 to 9) to a primary image dataset (phase 0) and analyzing the displacement in both translational and rotational directions. The study of dosimetric impacts from respiration includes both the effect of potential target and spinal cord motion and anatomic changes in the beam path. A clinical step-and-shoot IMRT plan generated on the free-breathing CT was copied to the 4-D datasets to evaluate the difference in the dose-volume histogram of target and normal tissues in each phase of a breathing cycle.

Results: Twenty three lesions had no motion in a breathing cycle; four lesions had anterior-posterior motion ≤ 0.2 mm; two lesions had lateral motion ≤ 0.2 mm; and eight lesions had superior-inferior motion, most ≤ 0.2 mm with the worst at 0.6 mm. The difference of maximum dose to 0.01 cm^3 of spinal cord in different phases of a breathing cycle was within 20 cGy in worst case. Target volumes that received the prescription dose (V100) varied little, with deviations of V100 of each phase from the average CT < 1% in most cases. Only when lesions were close to the diaphragm (e.g., at T11) did the V100 deviate by about 7% in the worst case scenario. However, this was caused by a small dose difference of 20 cGy to part of the target volume.

Conclusions: Breathing induced target and spinal cord motion is negligible compared with other setup uncertainties. Dose calculation using averaged or free-breathing CT is reliable when posterior beams are used.

Keywords: spinal SBRT, respiratory motion, 4-D CT

1. INTRODUCTION

Stereotactic body radiation therapy (SBRT) that delivers high dose in one or a few fractions is increasingly used to treat primary and metastatic disease in the spine. Such treatment provides a higher biologic equivalent dose than the conventional radiotherapy, which has been shown to provide better local control and pain relief (1). There are significant challenges in delivering a high dose, such as 24 Gy in a single fraction, to the spinal target while sparing the normal tissue in close proximity, such as spinal cord. One unique characteristic of spinal SBRT plan is the sharp drop off of dose between the target and normal tissues, which is typically ~2 Gy/mm (2). Consequently, spinal SBRT demands the highest accuracy in dose placement. In addition to sophisticated treatment planning system which can accurately model highly modulated small field beams, patient immobilization and multi-image guidance are indispensable components in achieving high accuracy of radiation delivery.

The uncertainties of initial set up and intra-fraction motion management of spinal SBRT are well understood (3-15). These results indicate accuracy of 1 to 2 mm can be achieved in initial setup. To maintain 2 mm accuracy through the treatment, intra-fraction monitoring and adjustment are also necessary since treatment delivery of spinal SBRT is a rather long process due to the high dose and complexity of the treatment. Most of the reported intra-fraction motion management studies were based on pre, middle and post treatment images, such as cone beam computed tomography (CBCT) or ExacTrac X-ray. The time between consecutive images in these studies was in minutes, which was much longer than a respiration cycle. Breathing-related motion of spinal targets is generally assumed to be minimum or non-existent in routine practice but rarely quantified and reported. Therefore, the purpose of this study was to use four-dimensional (4-D) computed tomography (CT) to evaluate the spinal target and spinal cord motion secondary to respiration and assess the potential dosimetric consequences from respiration.

The effect of motion on total dose distribution of a region of interest (ROI) treated with IMRT are categorized by Bortfeld et al (16) into 3 factors: 1) dose blurring as ROI moves within a stationary dose cloud; 2) interplay effects caused by the interplay between the motion of ROI and the motion of radiation beam defined by the multileaf collimator (MLC) aperture; 3) dose deformation due to anatomic changes. The first and second effects assumed the spatial dose distribution is invariant to displacements of the internal structures and of the whole patient. In other words, the ROI moves within a stationary "dose cloud" without affecting the cloud. If the ROI movement is not random, but treated as systematic positioning error, it does not cause dose blurring and interplay effect, but a shift of the dose distribution as a whole. In the third effect, stationary "dose cloud" is not valid anymore. Instead, the spatial dose distribution is altered by the anatomic change, such as the interface between structures of different densities moves in/out of the beam path. All these effects on target and organ at risk (OAR), which includes spinal cord dose/cauda equina, were assessed in worst scenario estimation in this work to make sure there is no surprise in the assumption of negligible dose perturbation from respiration in routine practice.

2. METHODS AND MATERIALS

2.1. Patient selection and simulation

Following multidisciplinary evaluation, patients dispositioned for spinal SBRT were offered inclusion on a prospective IRB-approved study (NCT01624220), as previously described (17). As per protocol, participants underwent an additional 4-D CT simulation scan at the time of treatment planning, in addition to the customary free-breathing scan.

Thirty patients with 33 lesions (3 C-spine, 20 T-spine and 10 L-spine) underwent treatment simulation in supine position in customized immobilization devices with both free-breathing and 4-D CT. A full body vacuum cushion (BodyFIX, Elekta) was molded to each patient to provide comfort and position reproducibility and stability. In addition, a thermoplastic mask (High Precision System for Head, Neck and Shoulders, Orfit) or plastic body cover sheet (BodyFIX, Elekta) was added for precise patient positioning and immobilization. The thermoplastic mask wrapped around the shoulder and covered most of the chest area. It was used for all

C-spine and most of upper T-spine (T1-T7) patients in the study. A Body cover sheet under vacuum was used on lower T, L and S spine patients. The arm position could be up over the head, wrapped above the chest or down by the side when the plastic cover sheet was used. The details of lesion location, radiation prescription and immobilization setup of each patient are summarized in Table 1.

Whence all the immobilization devices were made for a patient, a free-breathing CT simulation with 1 mm slice thickness was performed using multi slice helical CT (Brilliance Big Bore, Phillips). This CT dataset was used as the primary dataset to generate clinical treatment plan in Pinnacle (Philips Healthcare, Andover, MA). Immediately following the free-breathing CT, a 4-D CT scan was performed by wrapping a bellow belt around the abdominal region that tracked the breath volume change as a wave form. After identifying the peaks of the breath wave form (peak of inspiration) in the console software tool, 10 image datasets corresponding to 10 phases of a breathing cycle (0% to 90% by 10% increments, with 0% representing peak inspiration) were constructed in the temporal space. An averaged CT scan was also constructed from the 4-D data. Slice thickness was 2.5 mm for the 4-D CT. Resolution on the axial slices was <1.2 mm for all CT scans.

2.2. Target and spinal cord respiratory motion

Target respiratory motion was studied by registering a secondary image dataset (phase 10% to 90%) to a primary image dataset (phase 0%) in Pinnacle using the software registration setting of "CT to CT, normalized mutual information" with a 2 cm margin around the clinical target volume (CTV). The registration result included both the translational and rotational shifts, and its accuracy was manually verified using bony landmarks. Once the shift information of 9 phases was recorded, the largest translational and rotational motion in each direction between any 2 phases was calculated as the worst case scenario. The spinal cord/cauda equina was assumed to move with the boney target in this study. Thus, it had the same motion as the target.

2.3. Target and spinal cord dose perturbation due to their motion in a breathing cycle

A clinical step-and-shoot IMRT plan with 9 to 11 posterior beams (range from 100° to 280°) was generated in Pinnacle on free-breathing CT as previously described (2) for all patients except 1 (patient number 10) who underwent conventional 10-fraction treatment. Once the clinical plan was approved, it was copied to the 10 phases and average CT datasets, and dose was recalculated using the same isocenter, dose grid and monitor units. Since the target and spinal cord motion in a breathing cycle was very small and did not show any pattern in the "target and spinal cord respiratory motion" study of this work, we decided to treat the small breathing induced motion on target and spinal cord as a systematic error in the analysis of its dosimetrc impact. In the analysis, we shifted the target and OAR contours in both + and – direction with the value of the largest motion discovered in the "target and spinal cord respiratory motion" part of study, and examined the dose-volume histogram (DVH) change in plan calculated on the average CT. This is the worst scenario estimation comparing to dose blurring and interchange effect by random target and spinal cord motions. It assumed the motion stayed at maximum through the whole breathing cycle (like a setup error) to cause largest target underdose and OAR overdose.

2.4. Target and spinal cord dose perturbation due to dose deformation effect

In this analysis, both target and OARs, which includes spinal cord/cauda equina were assumed to be stable by using the same contours defined in the free breathing CT in the 4-D data sets. Therefore, the dosimetric impact was only due to potential breathing caused anatomic changes in the beam path, which could change the effective radiologic beam path length. The DVH data of Gross tumor volume (GTV), CTV and OAR in each phase were evaluated and compared with those on the average and free-breathing CT.

2.5. Dosimetric parameters for evaluating target and spinal cord dose pertubations

Tumor coverage at prescription dose level (percentage of tumor volume receiving prescription dose or higher [V100]) and 95% prescription dose level (V95) were used in this work to analyze the dosimetric impact to the target. These levels were chosen because they are at the sharp drop off region of DVH which is most likely to see the dosimetric impact, and both levels are commonly used by the clinician for plan evaluation. The maximal OAR dose was used to analyze the dosimetric impact to the spinal cord and caudal equina. It is defined as the greatest dose that at most 0.01 cm^3 of the OAR volume received and notated as D_{max}(0.01cc).

Table 1. List of patients, lesion location, immobilization setup, and prescription. It also includes the result of target motion study.

Patient No	Lesion Site	Immobilization	Prescribed Dose (Gy × Fractions)		Maximum Motion Between Any 2 Phases distance (mm), rotation (degree)
			GTV	CTV	
1	C5-7	M	24×1	16×1	None
2	C5-7	M	9×3	7×3	None
3	C6	M	9×3	7×3	None
4	T1	M	18×1	16×1	None
5	T1	M	18×1	16×1	None
6	T2	M	18×1	16×1	None
	T2	M	24×1	16×1	None
7	T6	M	24×1	16×1	None
8	T3	M	24×1	16×1	None
9	T2-4	M	24×1	16×1	0.2 AP
10	T5	SAH	NA	NA	0.2 SI
	T11	SAH	NA	NA	None
11	T6-7	SAH	6×5	5×5	None
12	T7	M	18×1	16×1	None
13	T7	SAH	18×1	16×1	0.2 SI, 0.2 AP
14	T8-9	SAH	24×1	16×1	None
15	T9	SAH	18×1	16×1	None
16	T9	SAH	24×1	16×1	None
17	T9	SAH	24×1	16×1	0.1 SI, 0.08 pitch
18	T10	SAC	24×1	16×1	0.6 SI
19	T11	SAH	18×1	18×1	0.15 yaw
20	T10-11	SAC	24×1	16×1	0.1 RL, 0.2 SI
21	T12	SAH	9×3	9×3	0.2 SI, 0.1 AP
22	L1	SAC	24×1	16×1	None
23	L1	SAC	24×1	16×1	None
24	L1-2	SAC	9×3	8×3	0.2 RL,0.2 AP, 0.1 SI
25	L2	SAC	24×1	16×1	None
	L2	SAC	24×1	16×1	None
26	L5	SAC	9×3	8×3	None
27	L3	SAC	24×1	16×1	None
28	L3	SAC	24×1	16×1	0.5 SI
29	L3	SAC	24×1	16×1	None
30	L3	SAC	18×1	16×1	None

Legend:
M= Mask
SAH = Plastic sheet with arms over head
SAC = Plastic sheet with arms on chest
AP = Anterior-posterior direction
RL = Lateral direction
SI = Superior-inferior direction

Table 2. Target motion in a breathing cycle for a T7 region lesion.

Phase	LR (mm)	AP (mm)	SI(mm)	Pitch (°)	Yaw (°)	Roll (°)
0%	baseline	baseline	baseline	baseline	baseline	baseline
10%	0	0	0	0	0	0
20%	0	-0.1	0.1	0	0	0
30%	0	0	0.1	0	0	0
40%	0	0	0.1	0	0	0
50%	0	-0.1	0	0	0	0
60%	0	0.1	0.1	0	0	0
70%	0	0.1	0.2	0	0	0
80%	0	0.1	0.1	0	0	0
90%	0	0	0	0	0	0

Legend:
AP = Anterior-posterior direction
RL = Lateral direction
SI = Superior-inferior direction

3. RESULTS

3.1. Target and spinal cord respiratory motion

All treatments were analyzed with respect to target motion throughout the respiratory cycle, as described above. The analysis of a representative lesion is illustrated in Table 2, which shows the registration results for a T7 lesion (patient number 13). Relative to phase 0%, this lesion exhibited a 0.1 mm superior-inferior (SI) motion at phase 20%, 30%, 40%, 60% and 80%, a 0.2 mm SI motion at phase 70%, a -0.1 mm anterior-posterior (AP) motion at phase 20% and 50%, and a 0.1 mm AP motion at phase 60%, 70% and 80%. Therefore, the largest translational and rotational motion in each direction between any 2 phases was taken as 0.2 mm SI and 0.2 mm AP. The results of such analysis on all lesions are summarized in Table 1. It shows that twenty three lesions had no motions in any direction. Two lesions had lateral motion ≤0.2 mm. Four lesions had AP motion ≤ 0.2 mm, and eight lesions had SI motion ≤ 0.6 mm with most (all but two) ≤ 0.2 mm. No discernable pattern or systematic deviation was evident, as exemplified by the T7 lesion data in Table 2.

3.2. Target and spinal cord dose perturbation due to their motion in a breathing cycle

Next, to analyze the potential impact of respiration induced motion on target coverage and OAR sparing, we assessed the consequences of the small motion discovered in the earlier motion analysis by assuming the motion as a systematic error. This is a worst scenario analysis by examining OARs shifting into higher dose region of the static dose cloud and target shifting into lower dose region of the static dose cloud. For the 9 lesions which showed motion in at least 1 direction in Table 1, Table 3 summarizes the worst scenario estimation of the 9 lesions. As expected, these small motions have minimal effect on the target coverage and OAR sparing. Most of them cause less than 0.5% difference in V100 and V95 with the worst being 1.5%. OAR Dmax(0.01cc) can be an extra 20 cGy in the worst case.

3.3. Target and spinal cord dose perturbation due to dose deformation effect

Finally, we sought to understand whether respiratory motion might potentially lead to changes in patient anatomy thus the beam radiologic path length, and whether these changes, unaccounted for by the planning CT dataset, might impact target coverage and OAR sparing. In Figure 1, examples are presented showing the dosimetric analysis of two lesions. Figure 1(a) shows the dosimetry result for a T11 lesion (patient number 19) which was prescribed 18 Gy in a single fraction to both CTV and GTV. It includes both the target coverage and cord sparing data calculated using the 4-D datasets with the assumption of stable targets and cord. The V100 of both GTV and CTV clearly shows that phase 0% and 60%

Table 3. Result of worst case scenario analysis of target (GTV and CTV) coverage and normal tissue sparing due to target motion. It includes the largest deficient of V100 and V95 of target and extra dose to normal tissue.

Patient No	Lesion site	Maximum Motion	Maximum GTV volume under dose (%)		Maximum CTV volume under dose (%)		Maximum OAR over dose (cGy)
			V100	V95	V100	V95	
9	T2-4	0.2 mm AP	-0.1	-0.0	-0.2	-0.2	10
		0.2 mm AP	-1.1	-0.9	-0.3	-0.3	10
13	T7	0.2 mm SI	-0.4	-0.2	-0.1	-0.1	0
17	T9	0.1 mm SI	-0.0	-0.0	-0.0	-0.0	0
		0.08° pitch	-0.0	-0.0	-0.0	-0.0	0
18	T10	0.6 mm SI	-1.5	-0.6	-1.5	-1.1	0
19	T11	0.15° yaw	-0.1	0.1	-0.1	0.1	20
20	T10-11	0.1 mm RL	-0.0	-0.0	-0.1	-0.1	20
		0.2 mm SI	-0.1	-0.0	-0.0	-0.0	0
21	T12	0.1 mm AP	-0.4	-0.2	-0.0	-0.0	10
		0.2 mm SI	-0.1	-0.0	-0.0	-0.0	5
24	L1-2	0.2 mm RL	-0.1	-0.1	-0.1	-0.1	15
		0.2 mm AP	-0.1	-0.1	-0.1	-0.1	10
		0.1 mm SI	-0.0	-0.0	-0.1	-0.0	0
28	L3	0.5 mm SI	-1.0	-0.5	-1.0	-0.5	0

Legend:
AP = Anterior-posterior direction
RL = Lateral direction
SI = Superior-inferior direction

of a breathing cycle has the best and worst target coverage respectively. The largest difference in V100 relative to average CT value is an underdose of approximately -6.5% for both GTV and CTV. V95 shows the same trend as V100, but the variation is flatter with the largest difference being about -1.1% from the average CT value for both GTV and CTV. This means that, relative to dose calculated using average CT and at the worst case of a breathing cycle, the target could have 6.5% less volume not receiving the prescription dose and 1% less volume not receiving 95% of the prescription dose. The OAR D_{max} (0.01cc) for this case ranges within 20 cGy of average CT value. Figure 1(b) shows the result of a T9 lesion (patient number 15). In contrast to the T11 lesion, it shows the V100 and V95 are almost constant throughout the breathing cycle. Relative to the average CT, Table 4 summarizes the largest possible underdose in target coverage and overdose in OAR sparing at a phase in a breathing cycle for lesions from T1 to L2. It includes all cases with lesion close to diaphragm (T7 to L1) and some of the upper T spine lesions randomly selected as representatives of that region. It shows that most cases are like the T9 lesion in Figure 1(b), with deviations of V100 and V95 of each phase from the average CT <0.5%. The T11 lesion presented in Figure 1(a) and a T8-9 lesion (patient number 14) are the only outliers. A DVH that includes phases 0%, 60% and average CT of the T11 case are plotted in Figure 2(a) for a closer look. It shows that, relative to the average CT, a small dose shift of ±20 cGy at the sharp drop-off region (near the prescription point) of the target DVH is responsible for the deviation of volume coverage. For this lesion, Figure 2(b) shows the variations of effective path length to isocenter along the beam central axis. It includes data for beam angles range from 0° (marked as 1 on x axis) to 340° (marked as 18 on x axis) in 20° increments. As expected for a posterior target, it shows the effective beam path length increases when beam angle rotate from posterior to anterior direction. It also shows a discontinuity at 260° and 280° with right lung in the beam path. The respiration motion of the interface at the right lung and liver also caused the largest variation of effective path length in a breathing cycle (6

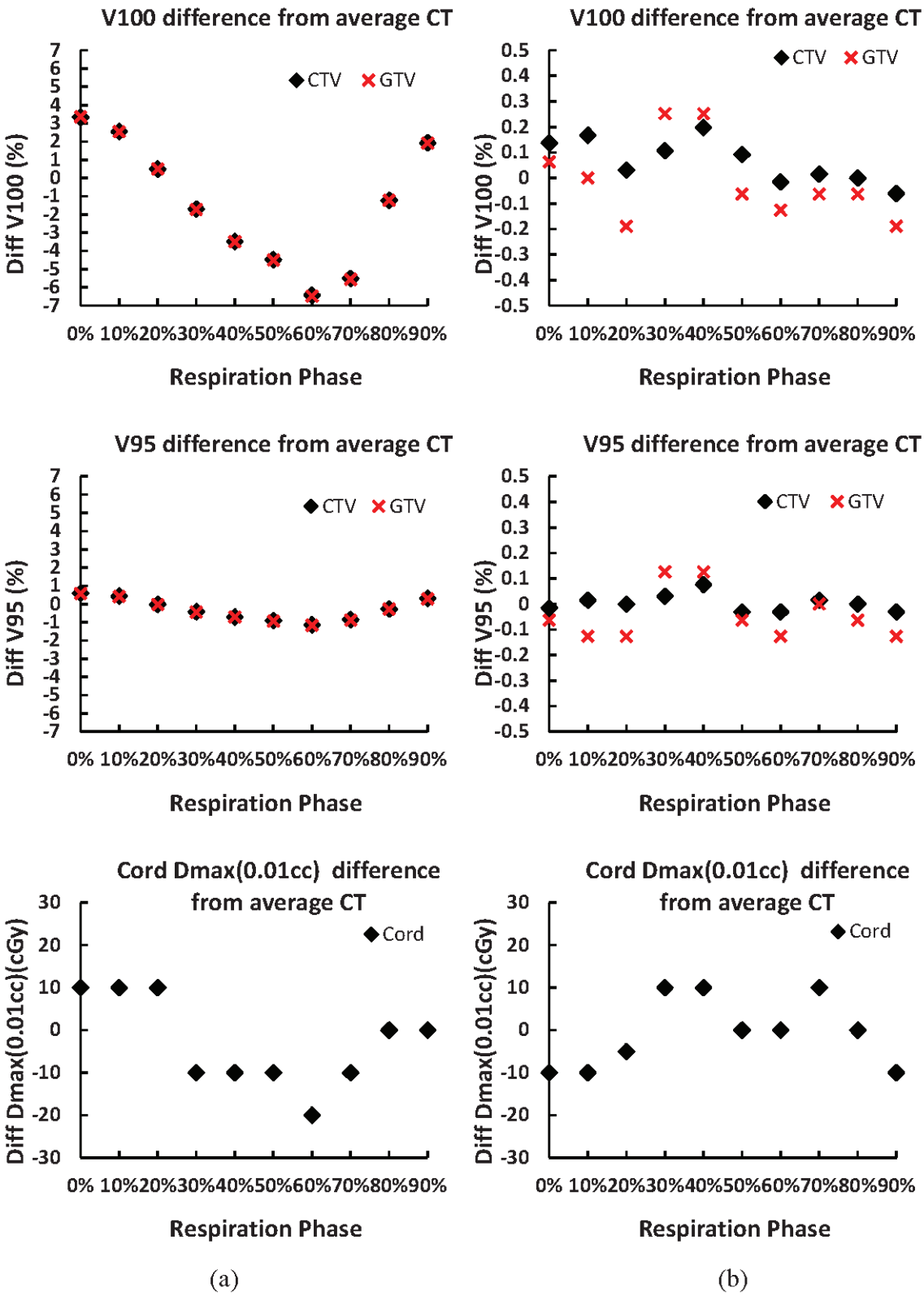

Figure 1. Difference of target coverage and spinal cord sparing in a breathing cycle from average CT. It includes V100 and V95 for both GTV and CTV and spinal cord D_{max}(0.01cc) data for two cases. T11 case (a) is on the left and T9 case (b) is on the right.

Table 4. Result of worst case scenario analysis of target (GTV and CTV) coverage and normal tissue sparing due to anatomical change associated with respiration. It includes the largest deficient of V100 and V95 of target and extra dose to normal tissue in any phase from the average CT value.

Patient No	Lesion Location	Maximum GTV volume under dose (%)		Maximum CTV volume under dose (%)		Maximum OAR over dose (cGy)
		V95	V100	V95	V100	
5	T1	-0.0	-0.1	-0.0	-0.0	0
6	T2	-0.1	-0.2	-0.0	-0.1	10
8	T3	-0.3	-0.3	-0.2	-0.2	20
7	T6	-0.2	-0.4	-0.1	-0.5	0
12	T7	-0.2	-0.2	-0.1	-0.1	10
13	T7	-0.0	-0.0	-0.0	-0.1	10
14	T8-9	-0.3	-7.5	-0.0	-0.1	0
15	T9	-0.1	-0.2	-0.0	-0.1	10
16	T9	-0.1	-0.2	-0.0	-0.1	10
17	T9	-0.0	-0.0	-0.0	-0.0	0
18	T10	-0.1	-0.1	-0.2	-0.0	0
19	T11	-1.2	-6.5	-1.1	-6.4	10
20	T10-11	-0.1	-0.3	-0.0	-0.0	10
21	T12	-1.1	-1.4	-0.8	-1.0	10
23	L1	-0.0	-0.0	-0.0	-0.0	10
24	L1-2	-0.0	-0.2	-0.0	-0.1	5

cm in 0% phase, 11 cm in 60% phase, 8.9 cm in average CT, and 6.6 cm in free breathing CT). Beams close to this angle used in the treatment planning is mostly responsible for the small dose difference in the DVH. OAR D_{max} (0.01cc) variation is small in a breathing cycle for all the patients, with most within 10 cGy and the worst at 20 cGy from the average CT value.

4. DISCUSSION

The safe and effective delivery of spinal SBRT requires meticulous attention to detail in the immobilization, planning and delivery of therapy. One source of possible intra-fraction error that has been potentially overlooked is the impact that respiratory motion during the breathing cycle might have dosimetric consequences for target coverage and OAR dose. In this study, patients were enrolled on a prospective protocol which included a 4D-CT simulation, allowing this question to be addressed.

The majority of lesions in the study had no motion in a breathing cycle. Some T and L spine lesions showed minimum motion in a few phases, with the largest being 0.6 mm in SI direction and 0.2 mm in lateral and AP direction. These motions also seem to happen randomly in the phases of a breath cycle which could suggest these measured deviations may be attributable to non-respiratory motion and its dosimetric impact can be conservatively estimated as a set up error. Considering the SI motions were less than the resolution of slice thickness (image registration error) and the magnitude of these values is much smaller than the typical 1 to 2 mm setup uncertainties, we believe the dosimetric impact associated with respiration is insignificant in our spinal SBRT practice. Our data also suggest the stability of spine in a breathing cycle is independent of the body positioning and immobilization device as various hand positions and immobilization setup were used in the study. We also looked randomly of 10 thorax patients outside of the patient group in this study who underwent 4-D simulation in a half body vacuum bag (BlueBag, Elekta) with hand over the head on a T-bar. The analysis of spine motion in these patients with relative minimum immobilization yielded the same result. In describing their experience of stereotactic body radiotherapy for lesions of the spine and paraspinal regisons, Nelson

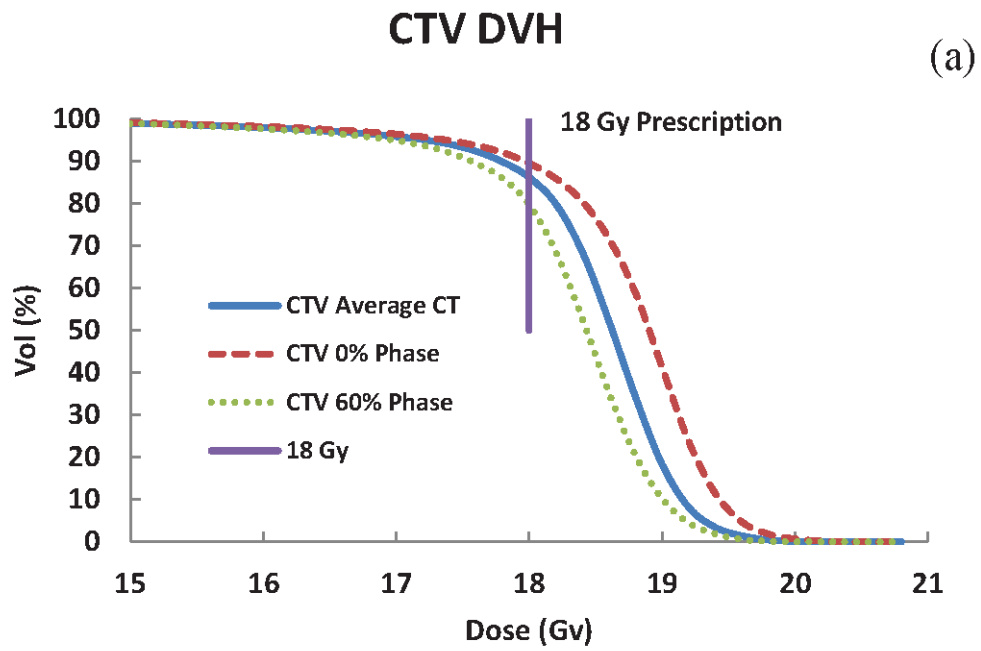

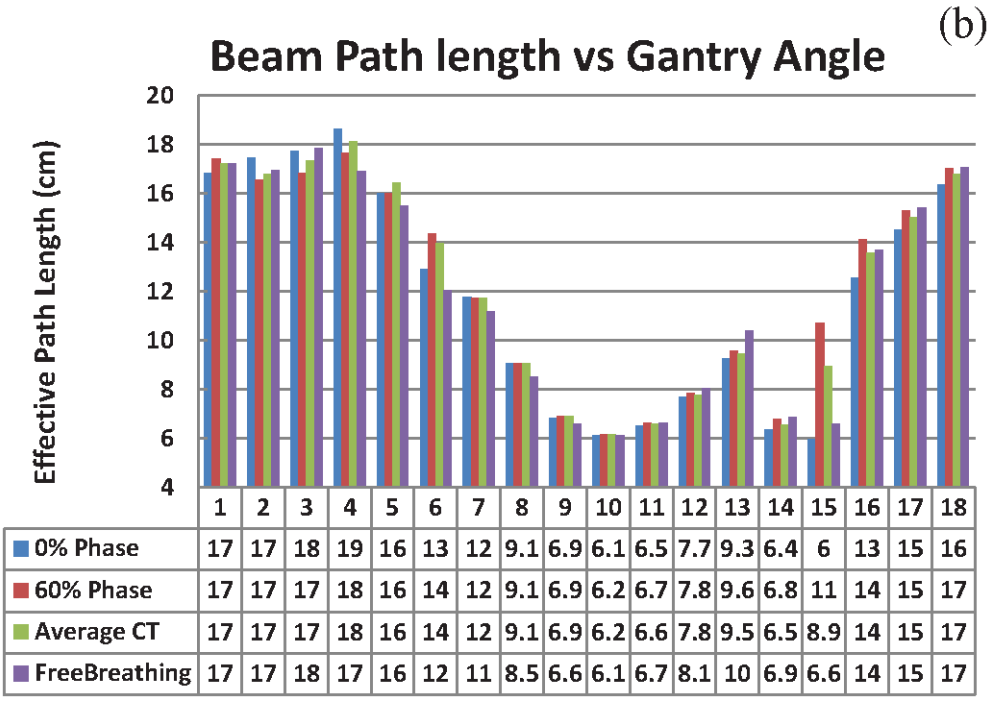

	1	2	3	4	5	6	7	8	9	10	11	12	13	14	15	16	17	18
0% Phase	17	17	18	19	16	13	12	9.1	6.9	6.1	6.5	7.7	9.3	6.4	6	13	15	16
60% Phase	17	17	17	18	16	14	12	9.1	6.9	6.2	6.7	7.8	9.6	6.8	11	14	15	17
Average CT	17	17	17	18	16	14	12	9.1	6.9	6.2	6.6	7.8	9.5	6.5	8.9	14	15	17
FreeBreathing	17	17	18	17	16	12	11	8.5	6.6	6.1	6.7	8.1	10	6.9	6.6	14	15	17

Figure 2. (a) is the DVH of CTV of a T11 case. It includes the data for phase 0%, 60% and average CT. (b) is the effective path length to isocenter along the beam central axis for 0%, 60%, average and free breathing CT. It covers beam angle from 0° to 340° in 20° increments (marked as 1 to 18 in x axis).

et al (8) also mentioned (without presenting any data) that the first 10 patients simulated with 4-D CT showed stable axial skeleton positioning. These results suggest that the spine by nature is not a moving component during respiration. The custom made full body cradle acts as the primary immobilization apparatus to reproduce accurate patient position and reduce voluntary intra fraction motion.

Hypothetically, dosimetric perturbation to the target and OAR at different phase of a breathing cycle could be grouped into 2 categories: 1) motion of target and OAR relative to the beam, which includes both dose blurring and interplay effect; 2) the effective radiologic beam path length change associated with anatomy change. Category 1 is negligible since the respiration of target and spinal cord can be ignored. Diaphragm motion can change the radiologic beam path length by moving dense tissue in and out of a beam path. It mainly affects the more lateral beams and has higher impact on the anterior part of the target. This is demonstrated by the T11 lesion which has the best target coverage at phase 0% (peak of inhale, dense tissue moving out of the beam path) and the worst coverage at phase 60% (close to the end of exhale, dense tissue moving into the beam path) . The cord dose varied little because it is more posterior. A close look of the DVH for this case in Figure 2 revealed the 10% deviation of target volume that received prescription dose between the best and worst coverage was caused by a small dose shift of 40 cGy (2% of prescription dose) at the sharp drop-off region (near the prescription point) of the target between 2 phases. This small dose difference is even smaller when averaged through the treatment process. This worst case analysis also indicates that dose calculated using free breathing CT reflects the delivered dose, even if we assume the free breathing CT is close to 0% data set, and deliver is over 60% phase data set (most likely average CT).

Overall, our analysis shows that most clinical cases with posterior beams are not affected by the diaphragm motion at all, and our results support the use of average or free breathing data sets as for planning. Our data also indicated that diaphragm motion can significantly change the effective path length of some lateral beams. For plans with high weighting on the lateral beams, a comparison of planning CT and setup cone beam CT can help on the estimation of dose perturbations from anatomic change.

5. CONCLUSION

Target and spinal cord motion associated with breathing is negligible comparing with other factors like setup uncertainties and intra fraction motion. Dose calculation using average or free breathing CT is reliable when posterior beams are used for spinal SBRT treatment.

Authors' disclosure of potential conflicts of interest

The authors reported no conflict of interest.

Author contributions

Conception and design: David Weksberg, Eric Chang, Amol Ghia, Paul Brown, James Yang
Data collection: Xin Wang, Amol Ghia, Zhongxiang Zhao, Jinzhong Yang, Dershan Luo, Tina Briere, Jing Li, Mary McAleer, David Weksberg, Eric Chang, Paul Brown, James Yang, Ramiro Pino
Data analysis and interpretation: Xin Wang, Amol Ghia, Zhongxiang Zhao, Jinzhong Yang, Dershan Luo, Tina Briere, Ramiro Pino, Jing Li, Mary McAleer, David Weksberg, Eric Chang, Paul Brown, James Yang
Manuscript writing: Xin Wang, Amol Ghia, Zhongxiang Zhao, Jinzhong Yang, Dershan Luo, Tina Briere, Jing Li, Mary McAleer, David Weksberg, Eric Chang, Paul Brown, James Yang
Final approval of manuscript: James Yang

REFERENCES

1. Garg, AK, Shiu AS, Yang J, Wang XS, Allen P, Brown BW, Grossman P, Frija EK, McAleer MF, Azeem S, Brown PD, Rhines LD, Chang EL. (2012). Phase 1/2 trial of single-session stereotactic body radiotherapy for previously unirradiated spinal metastases. *Cancer*, 118, 5069-77.
2. Weksberg DC, Palmer MB, Vu KN, Rebueno NC, Sharp HJ, Luo D, Yang JN, Shiu AS, Rhines LD, McAleer MF, Brown PD, Chang EL. (2012). Generalizable class solutions for treatment planning of spinal stereotactic body radiation therapy. *Int J Radiat Oncol Biol Phys*, 84, 847-53.
3. Yin FF, Ryu S, Ajlouni M, Zhu J, Yan H, Guan H, Faber K, Rock J, Abdalhak M, Rogers L, Rosenblum M, Kim JH. (2002). A technique of intensity-modulated radiosurgery (IMRS) for spinal tumors. *Med Phys*, 29, 2815-22.
4. Murphy MJ, Chang SD, Gibbs IC, Le QT, Hai J, Kim D, Martin DP, Adler JR Jr. (2003). Patterns of patient movement during frameless image-guided radiosurgery. *Int J Radiat Oncol Biol Phys*, 55, 1400-8.
5. Chuang C, Sahgal A, Lee L, Larson D, Huang K, Petti P, Verhey L, Ma L. (2007). Effects of residual target motion for image-tracked spine radiosurgery. *Med Phys*, 34, 4484-90.
6. Hoogeman MS, Nuyttens JJ, Levendag PC, Heijmen BJ. (2008). Time dependence of intrafraction patient motion assessed by repeat stereoscopic imaging. *Int J Radiat Oncol Biol Phys*, 70, 609-18.
7. Agazaryan N, Tenn SE, Desalles AA, Selch MT. (2008) Image-guided radiosurgery for spinal tumors: methods, accuracy and patient intrafraction motion. *Phys Med Biol*, 53, 1715-27.
8. Jin JY, Ryu S, Rock J, Faber K, Chen Q, Ajlouni M, Movsas B. (2008). Evaluation of residual patient position variation for spinal radiosurgery using the Novalis image guided system. *Med Phys*, 35, 1087-93.
9. Nelson JW, Yoo DS, Sampson JH, Isaacs RE, Larrier NA, Marks LB, Yin FF, Wu QJ, Wang Z, Kirkpatrick JP. (2009). Stereotactic body radiotherapy for lesions of the spine and paraspinal regions. *Int J Radiat Oncol Biol Phys*, 73, 1369-75.
10. Kim S, Jin H, Yang H, Amdur RJ. (2009). A study on target positioning error and its impact on dose variation in image-guided stereotactic body radiotherapy for the spine. *Int J Radiat Oncol Biol Phys*, 73, 1574-9.

11. Ma L, Sahgal A, Hossain S, Chuang C, Descovich M, Huang K, Gottschalk A, Larson DA. (2009). Nonrandom intrafraction target motions and general strategy for correction of spine stereotactic body radiotherapy. *Int J Radiat Oncol Biol Phys*, 75, 1261-5.

12. Gerszten PC, Monaco EA 3rd, Quader M, Novotny J Jr, Kim JO, Flickinger JC, Huq MS. (2010). Setup accuracy of spine radiosurgery using cone beam computed tomography image guidance in patients with spinal implants. *J Neurosurg Spine*, 12, 413-20.

13. Hyde D, Lochray F, Korol R, Davidson M, Wong CS, Ma L, Sahgal A. (2012). Spine stereotactic body radiotherapy utilizing cone-beam CT image-guidance with a robotic couch: intrafraction motion analysis accounting for all six degrees of freedom. *Int J Radiat Oncol Biol Phys*, 82, 555-62.

14. Li W, Sahgal A, Foote M, Millar BA, Jaffray DA, Letourneau D. (2012). Impact of immobilization on intrafraction motion for spine stereotactic body radiotherapy using cone beam computed tomography. *Int J Radiat Oncol Biol Phys*, 84, 520-6.

15. Yamoah K, Zaorsky NG, Siglin J, et al. Spine Stereotactic Body Radiation Therapy Residual Setup Errors and Intra-Fraction Motion Using the Stereotactic X-Ray Image Guidance Verification System. *Int J Med Phys Clin Engr Radiat Oncl* 2014;3:1-8.

16. Bortfeld T, Jiang SB, Rietzel E. (2004). Effects of motion on the total dose distribution. *Semin Radiat Oncol*, 14, 41-51.

17. Weksberg DC, Yang JN, Tam AL, Li J, Wang XA, Zhao Z, Mcrae SE, Settle SH, Rhines LD, Chang EL, Brown PD, Ghia AJ. (2016), Prospective validation of treatment accuracy using implanted fiducial markers for spinal stereotactic body radiation therapy. *J Radiosurg SBRT*, 4, 7-14.